

# Gravitational Rutherford scattering and Keplerian orbits for electrically charged bodies in heterotic string theory

J. R. Villanueva<sup>a,1,2</sup>, Marco Olivares<sup>b,3</sup>

<sup>1</sup>Instituto de Física y Astronomía, Universidad de Valparaíso, Gran Bretaña 1111, Valparaíso, Chile

<sup>2</sup>Centro de Astrofísica de Valparaíso, Gran Bretaña 1111, Playa Ancha, Valparaíso, Chile

<sup>3</sup>Facultad de Ingeniería, Universidad Diego Portales, Avenida Ejército Libertador 441, Casilla 298-V, Santiago, Chile

Received: XX XXXX 201X / Accepted: XX XXXX 201X

**Abstract** Properties of the motion of electrically charged particles in the background of the Gibbons–Maeda–Garfinkle–Horowitz–Strominger (GMGHS) black hole is presented in this paper. Radial and angular motion are studied analytically for different values of the fundamental parameter. Therefore, *gravitational Rutherford scattering* and *Keplerian orbits* are analysed in detail. Finally, this paper complements previous work by Fernando for null geodesics (Phys. Rev. D **85**: 024033, 2012), Olivares & Villanueva (Eur. Phys. J. C **73**: 2659, 2013) and Blaga (Automat. Comp. Appl. Math. **22**, 41 (2013); Serb. Astron. J. **190**, 41 (2015)) for time-like geodesics.

**PACS** 04.20.Fy, 04.20.Jb, 04.40.Nr, 04.70.Bw

## Contents

1	Introduction . . . . .	1
2	Charged black holes in heterotic string theory . . . . .	2
3	Motion of charged particles . . . . .	3
4	Radial trajectories . . . . .	3
5	Motion with angular momentum . . . . .	6
6	Final remarks . . . . .	8

## 1 Introduction

The study of the motion of test particles around compact objects is one interesting way to probe some phenomena related to classic tests of the general relativity. In the context of Einstein gravity, orbital precession experienced by the solar planets, particularly Mercury, and the deflection of light was studied earlier by Einstein himself [1, 2] and other renowned scientists [3, 4]. Nearly a century after of them, a lot of research has been conducted on these tests together with other

studies (time delay, strong gravity, gravitational waves, etc.). Fundamentals and current advances can be found, for example, in [5, 6].

In other spacetimes containing black hole solutions, the motion of particles has also received a great deal of attention from the physics community. For instance, a review of neutral massive and massless particles moving in the background of the Schwarzschild (S), Reissner-Nordström (RN) and Kerr (K) black holes can be found in [7]. Furthermore, the inclusion of a cosmological constant  $\Lambda$  leads to the Kottler solution [8], which spacetime is known as the Schwarzschild de Sitter (SdS) if  $\Lambda > 0$ , or the Schwarzschild anti-de Sitter (SAdS) if  $\Lambda < 0$ . So, trajectories for neutral particles in a purely SdS spacetime can be found in [9–12], while different aspects of the motion of neutral particles in the background of the purely SAdS spacetime has been presented in [13–18]. Uncharged particles in RN black hole with  $\Lambda \neq 0$  was studied by Stuchlík & Hledík [19], whereas circular orbits was presented by Pugliese et al. [20]. Furthermore, Hackmann et al. [21] presents analytical solutions of the geodesic equation of massive test particles in higher dimensional Schwarzschild, Schwarzschild anti-de Sitter, Reissner Nordström, and Reissner Nordström anti-de Sitter (RNAdS) spacetimes and they obtained complete solutions and a classification of the possible orbits in these geometries in term of Weierstraß functions. Also, bounded time-like geodesics in Kerr (K) spacetime are found in [22], whereas equatorial circular motion in Kerr–de Sitter (KdS) and Kerr-Newman (KN) spacetimes was performed by Stuchlík & Slany [23] and by Pugliese et al. [24], respectively.

There is just as much literature dealing with alternatives theories of gravitation. In fact, here we mention only a few studies dealing with the motion of neutral particles. For example, in conformal Weyl gravity, there are many articles studying the motion of particles in addition to some observational tests [25–29], similar to those for asymptotically

<sup>a</sup>e-mail: jose.villanuevalob@uv.cl

<sup>b</sup>e-mail: marco.olivaresr@mail.udp.cl

Lifshitz spacetimes [30–34]. The complete causal structure of the Bardeen spacetime was presented in [35], the Rindler modified Schwarzschild geodesics in [36], while the Schwarzschild version in gravity’s Rainbow was performed by Leiva et al. [37]. Not least are the contributions from string theories. Here we can mention the works of Maki & Shiraishi [38], Hackmann et al. [39], Hartmann & Sirimachan [40] and Bhadra [41], among other authors.

The motion of electrically charged particles represents another current line of investigation, which posits interesting features due to the extra interaction between the particle and the electromagnetic field of the background. In this sense, trajectories in a dipole magnetic field and in a toroidal magnetic field on the Schwarzschild background were performed by Prasanna & Varma and Prasanna & Sengupta [42, 43], respectively, whereas Dadhich et al. [44] made calculations for trajectories on the same background when the black hole is immersed in an axially symmetric magnetic field (Ernst spacetime). The general features of radial motion, motion along the axis of symmetry and motion on the equatorial plane in the field of rotating charged black holes was performed in two parts by Balek, Bičák & Stuchlík [45, 46]. Relativistic radial motion of electrically charged particles in the field of a charged spherically symmetric distribution of mass can be found in [47], whereas classical electrically and magnetically charged test particles in the same spacetime were made by Grunau and Kagramanova [48]. Trajectories on the RN black hole were performed by Cohen & Gautreau and Pugliese et al. when  $\Lambda = 0$  [49, 50], and by Olivares et al. when  $\Lambda < 0$  (RNAdS) [51]. The motion on a rotating Kerr black hole immersed in a magnetic field has been studied by Aliev & Özdemir [52] and by Takahashi & Koyama [54], the non-Kerr rotating version by Abdurjabbarov [53], finally the Kerr-Newmann background has been covered by Hackmann & Xu [55].

The main goal of this paper is to work out the motion of electrically charged particles on the spacetime of a black hole coming from the heterotic string theory, the so-called GMGHS black hole, the causal structure of which has been determined by Fernando for null geodesic [56], and by Olivares & Villanueva [57] and Blaga [58, 59] for time-like geodesics. In this article we use natural units with  $c = 1$  and  $G = 1$ , together with the value of the heterotic parameter found earlier in [57],  $\alpha = 0.359$  [Km]. Therefore, in Section 2 the charged black hole in heterotic string theory is presented, in Section 3 the fundamental equations of motion for electrically charged particles are obtained using the Hamilton–Jacobi method. In Section 4 we perform a full analysis of the radial motion of test particles, and in Section 5 we solve angular trajectories analytically and we study the gravitational scattering of Rutherford in detail. Finally, in section 6 we conclude with general comments and final remarks.

## 2 Charged black holes in heterotic string theory

The simplest 4-dimensional black hole solutions in heterotic string theory, which contain mass and electric charge, are obtained from the effective action [60]

$$\mathcal{I}_{hst} = \frac{1}{16\pi} \int d^4x \sqrt{-g} [R - 2(\nabla\Phi)^2 - e^{-2\Phi} F_{\mu\nu} F^{\mu\nu}], \quad (1)$$

where  $\Phi$  is the dilaton field,  $R$  is the scalar curvature and  $F_{\mu\nu} = \partial_\mu A_\nu - \partial_\nu A_\mu$  is the Maxwell’s field strength associated with a  $U(1)$  subgroup of  $E_8 \times E_8$  or  $\text{Spin}(32)$  [60, 61]. The field equations associated with this action read

$$\nabla_\mu (e^{-2\Phi} F^{\mu\nu}) = 0, \quad (2)$$

$$\nabla^2 \Phi + \frac{1}{2} e^{-2\Phi} F^2 = 0, \quad (3)$$

and

$$R_{\mu\nu} = -2\nabla_\mu \Phi \nabla_\nu \Phi - 2e^{-2\Phi} F_{\mu\lambda} F_\nu^\lambda + \frac{1}{2} g_{\mu\nu} e^{-2\Phi} F^2, \quad (4)$$

and were solved by Gibbons & Maeda [62], and independently by Garfinkle, Horowitz & Strominger [63], and thus this is known as the Gibbons–Maeda–Garfinkle–Horowitz–Strominger (GMGHS) black hole, whose metric in the Einstein frame is given by [56, 57]

$$ds^2 = -\mathcal{F}(r) dt^2 + \frac{dr^2}{\mathcal{F}(r)} + \mathcal{R}^2(r) (d\theta^2 + \sin^2 \theta d\phi^2). \quad (5)$$

Here the coordinates are defined in the ranges  $0 < r < \infty$ ,  $-\infty < t < \infty$ ,  $0 \leq \theta < \pi$ ,  $0 \leq \phi < 2\pi$ , and the radial function  $\mathcal{R}(r)$  is given by

$$\mathcal{R}(r) = \sqrt{r(r-\alpha)}, \quad \alpha \equiv \frac{Q^2}{M}, \quad (6)$$

where  $M$  is the ADM mass,  $Q$  is the electric charge, and  $\mathcal{F}(r)$  is the well-known lapse function of the Schwarzschild black hole,

$$\mathcal{F}(r) = 1 - \frac{2M}{r} = 1 - \frac{r_+}{r}, \quad r_+ = 2M. \quad (7)$$

Since the coordinates  $(t, \phi)$  are cyclic in the metric (5), there are two conserved quantities related to two Killing vectors fields:

- the *time-like Killing vector*  $\xi_t = (1, 0, 0, 0)$  is related to the *stationarity* of the metric:  $g_{\alpha\beta} \xi_t^\alpha u^\beta = -\mathcal{F}(r) \dot{t} = -\sqrt{E}$  is a constant of motion which can be associated with the total energy of the test particles, because this spacetime is asymptotically flat, and
- the *space-like Killing vector*  $\xi_\phi = (0, 0, 0, 1)$  is related to the axial symmetry of the metric:  $g_{\alpha\beta} \xi_\phi^\alpha u^\beta = \mathcal{R}^2(r) \sin^2 \theta \dot{\phi} = L$  is a constant of motion corresponding to the angular momentum of the particles moving in this geometry.

With all this, in the next section the basic equations governing the motion of charged particles in the spacetime generated by the GMGHS black hole are obtained by using the Hamilton–Jacobi formalism.

### 3 Motion of charged particles

Let us consider the motion of test particles which possess mass  $m$  and electric charge  $\tilde{q}$ . The Hamilton–Jacobi equation for the geometry described by the metric  $g_{\mu\nu}$  is given by

$$\frac{1}{2}g^{\mu\nu}\left(\frac{\partial S}{\partial x^\mu} + \tilde{q}A_\mu\right)\left(\frac{\partial S}{\partial x^\nu} + \tilde{q}A_\nu\right) + \frac{\partial S}{\partial \tau} = 0, \quad (8)$$

where  $S$  corresponds to the characteristic Hamilton function and  $A_\mu$  represents the vector potential components associated with the electrodynamic properties of the black hole. Since we are considering charged static black holes, the only non-vanishing component of the vector potential is the temporal,  $A_t = Q/r$ . Also, the conservation of the angular motion implies that the motion is developed on an invariant plane, which we choose to be  $\theta = \pi/2$ , so Eq. (8) reads

$$-\frac{1}{\mathcal{F}}\left(\frac{\partial S}{\partial t} + \frac{\tilde{q}}{r}\sqrt{\frac{\alpha r_+}{2}}\right)^2 + \mathcal{F}\left(\frac{\partial S}{\partial r}\right)^2 + \frac{1}{\mathcal{R}^2}\left(\frac{\partial S}{\partial \phi}\right)^2 + 2\frac{\partial S}{\partial \tau} = 0. \quad (9)$$

Aiming to solve this last equation, we introduce the ansatz  $S = -Et + S_0(r) + L\phi + \frac{1}{2}m^2\tau$ , together with the re-definition of the test charge  $q = \tilde{q}\sqrt{\frac{\alpha r_+}{2}}$ , and thus rewrite it as

$$S_0(r) = \pm \int \frac{dr}{\mathcal{F}} \sqrt{(E - V_-)(E - V_+)}, \quad (10)$$

where the radial functions are given by

$$V_\pm(r) = V_q(r) \pm \sqrt{\mathcal{F}\left(m^2 + \frac{L^2}{\mathcal{R}^2}\right)}, \quad V_q(r) \equiv \frac{q}{r}. \quad (11)$$

Notice that each branch converges to the value  $E_+ = q/r_+$  at  $r = r_+$ , which can be either positive or negative, depending on the sign of the electric charge. In Fig. 1 we show the  $q > 0$  case in which the  $V_-$  branch always is negative (except in the region  $r_+ < r < r_q$ , where  $r_q$  is solution to the equation  $V_-(r_q) = 0$ ). From now on we will call the positive branch  $V_{eff} = V_+ \equiv V$  effective potential.

Employing the Hamilton-Jacobi method, it is possible to obtain three velocities taking into account the motion of test particles. So, by making  $\frac{\partial S}{\partial m^2} = 0$ ,  $\frac{\partial S}{\partial E} = 0$ , and  $\frac{\partial S}{\partial L} = 0$ , we obtain

$$u(r) \equiv \frac{dr}{d\tau} = \pm \sqrt{(E - V_-)(E - V)}, \quad (12)$$

$$v_t(r) \equiv \frac{dr}{dt} = \pm \frac{\mathcal{F}(r)u(r)}{E - V_q(r)}, \quad (13)$$

and

$$v_\phi(r) = \frac{dr}{d\phi} = \pm \frac{\mathcal{R}^2(r)u(r)}{L}, \quad (14)$$

respectively. Notice that the zeros in Eq. (12), and therefore of Eqs. (13) and (14), correspond to the so-called turning point,  $r_t$ . Furthermore, these equations lead to the quadratures that determine the evolution of the electrically charged test particles, so next sections are devoted to obtaining their analytical solutions.

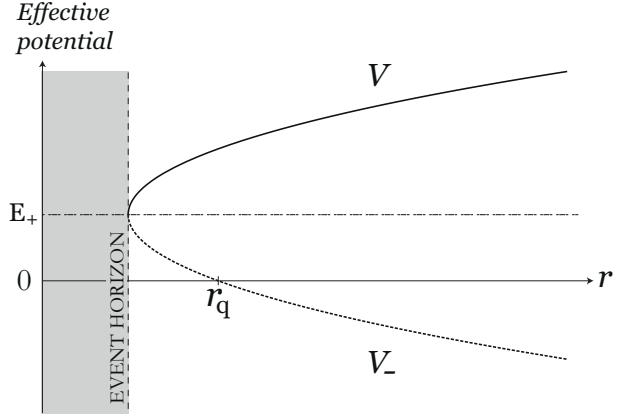


**Fig. 1** Plot of the effective potential  $V(r)$  for positive charged particles ( $q > 0$ ) in radial motion together with the negative branch  $V_-(r)$ , which is positive in the range  $r_+ < r < r_q$ . Also, at the event horizon  $r_+$ , each branch converges to  $E_+ = q/r_+$ .

### 4 Radial trajectories

The radial motion of charged particles is characterized by the condition  $L = 0$ , in which case the effective potential becomes

$$V(r) = V_q(r) + m\sqrt{\mathcal{F}(r)}. \quad (15)$$

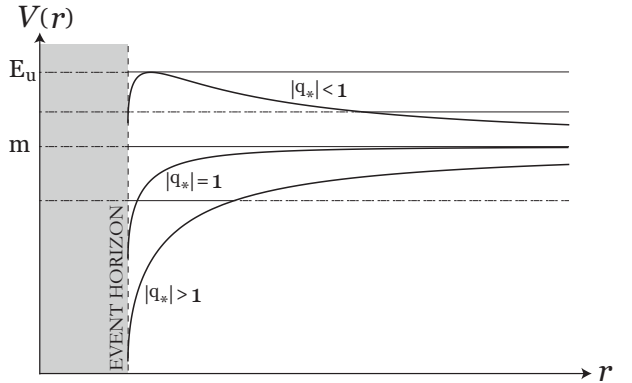


**Fig. 2** Typical graphs of the effective potential as a function of the radial coordinate. Here, we show the curves in terms of the *electric ratio*  $q_* = q_c/q$ , where  $q_c = mr_+/2$ . Notice that if  $|q_*| < 1$  and  $m < E < E_u$  a frontal scattering is permitted. For  $|q_*| \geq 1$ , the motion is essentially the same as in the Schwarzschild case.

In Fig. 2 the effective potential (15) for three different values of the electric charge is shown. A first observation of this graph is that effective potential presents two well defined behaviors in the region  $r_+ < r < \infty$ :

*the classic domain* is characterized by the absence of a maximum, so that particles with  $E < m$  inexorably fall to the event horizon, whereas if  $E > m$ , particles can escape (fall) into the spatial infinity (event horizon). Essentially, the neutral particles exhibit this same behavior in this spacetime,

which, as has been pointed out in [57], corresponds to the typical motion in the background of a Schwarzschild black hole. In Fig. 2, the two lower curves correspond to this domain.

The *electric domain* allows a maximum equal to  $E_u = E_+ (1 + q_*^2)$ , where  $q_* = q_c/q$  is the electric ratio and  $q_c = mr_+/2$ . Therefore, particles with  $m < E < E_u$  feel a radial repulsion and cannot fall into the event horizon. Furthermore, as in the previous case, if  $E > E_u$ , particles can escape (fall) into the spatial infinity (event horizon). This domain is represented by the upper curve in Fig. 2.

The extreme of the effective potential is located at  $\rho_u = \frac{r_+}{1 - q_*^2}$ , (16)

so we can conclude that if  $|q_*| < 1$ , then the position of the maximum is in the region  $[r_+, \infty]$ , while if  $|q_*| > 1$ , then the location of the maximum is in the region  $[-\infty, 0]$ ; finally, if  $q_* = 1$ , then the potential has no maximum.

Ultimately, in order to simplify the calculations, it is instructive to rewrite square of the proper velocity (12) in the generic form:

$$\begin{aligned} u^2(r) &= (E - V)(E - V_-) \\ &= \left( \frac{m^2 - E^2}{r^2} \right) \left[ \frac{q^2}{m^2 - E^2} + \frac{2q(mq_* - E)}{m^2 - E^2} r - r^2 \right] \\ &\equiv \left( \frac{m^2 - E^2}{r^2} \right) p_2(r), \end{aligned} \quad (17)$$

and thus, an exhaustive study of the radial motion can be carried out taking account the values of the fundamental parameters.

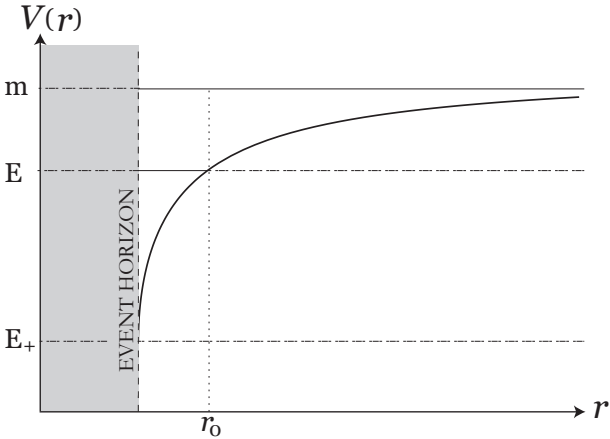


**Fig. 3** Plot of the effective potential for radial charged particles in the classic domain. Bounded trajectories: particles with electric ratio  $|q_*| > 1$  and energy  $E_+ < E < m$  cannot escape to spatial infinity, so the distance  $r_0$  corresponds to a turning point. Unbounded trajectories: particles with electric ratio  $|q_*| = 1$  and energy  $m < E < E_\infty$  arrive to spatial infinity with non-vanished kinetic energy  $K \geq 0$ . For simplicity, because the motion is essentially the same for all  $E \in \{m, E_\infty\}$ , here we solve the case  $E = m$  and the starting point  $r_0$  has been chosen in such way that  $t(r_0) = \tau(r_0) = 0$ .

#### 4.1 The classic domain

As we have said, basically this domain is analogous to the Schwarzschild counterpart [7]. It is important to note that electric interaction is weak with respect to gravitational effects, so charged particles behave like neutral particles as we have seen pointed out in Ref. [57].

##### 4.1.1 bounded trajectories : $|q_*| > 1$ and $E_+ < E < m$

In this case, as shown in Fig. 3, we write the polynomial as  $p_2(r) = (r_0 - r)(r - d_0)$ , where

$$r_0 = \frac{1}{2} (b + \sqrt{b^2 + 4a}), \quad d_0 = \frac{1}{2} (b - \sqrt{b^2 + 4a}), \quad (18)$$

$$a = \frac{q^2}{m^2 - E^2}, \quad b = 2q \left( \frac{mq_* - E}{m^2 - E^2} \right). \quad (19)$$

Inserting this polynomial into Eq. (17), and then integrating Eqs. (12) and (13), we obtain that the proper time is given by

$$\tau(r) = \frac{\sqrt{p_2(r)} + g(0) \left[ \arctan \left( \frac{g(r)}{\sqrt{p_2(r)}} \right) - \frac{\pi}{2} \right]}{\sqrt{m^2 - E^2}}, \quad (20)$$

while the coordinate time becomes

$$t(r) = \left[ E + \frac{q}{g(0)} \left( \frac{E}{E_+} - 1 \right) \right] \tau(r) + \mathcal{F}(r), \quad (21)$$

where

$$\mathcal{F}(r) = a \left( \frac{E}{E_+} - 1 \right) \left[ \frac{r_+}{\sqrt{p_2(r_+)}} \log \left( \frac{(r-r_+)g(r_0)}{r_+r+r_0d_0-(r+r_+)g(0)} \right) - \frac{\sqrt{p_2(r)}}{g(0)} \right], \quad (22)$$

where  $g(r) = \frac{1}{2}[(r_0 - r) - (r - d_0)]$ , and we must choose  $\tau(r_0) = t(r_0) = 0$ . In top panel of Fig. 4 the functions (20) and (21) are plotted together, demonstrating that radial charged particles present the same behavior as radial neutral particles in this spacetime [57].

##### 4.1.2 unbounded trajectories : $q_* = 1$ and $E \geq m$

This case is characterized by the possibility that particles can arrive to spatial infinity with non-null kinetic energy,  $K \geq 0$ , where the equality is satisfied when  $E = m$ , see Fig. 3. Thus, for simplicity, we solve this last case so the proper and coordinate velocity becomes

$$u(r) \equiv u_c(r) = \pm \frac{q_c}{r}, \quad (23)$$

and

$$v_t(r) = \pm \frac{(1 - \frac{2}{m}u_c)u_c}{m - u_c} \quad (24)$$

For simplicity, let us choose  $r_0$  as the starting distance, where  $\tau(r_0) = t(r_0) = 0$ ; therefore, Eqs. (23) and (24) become

$$\tau(r) = \pm \frac{r^2 - r_0^2}{2q_c}, \quad (25)$$

and

$$t(r) = m\tau(r) \pm (r - r_0) \pm r_+ \ln \left( \frac{r - r_+}{r_0 - r_+} \right), \quad (26)$$

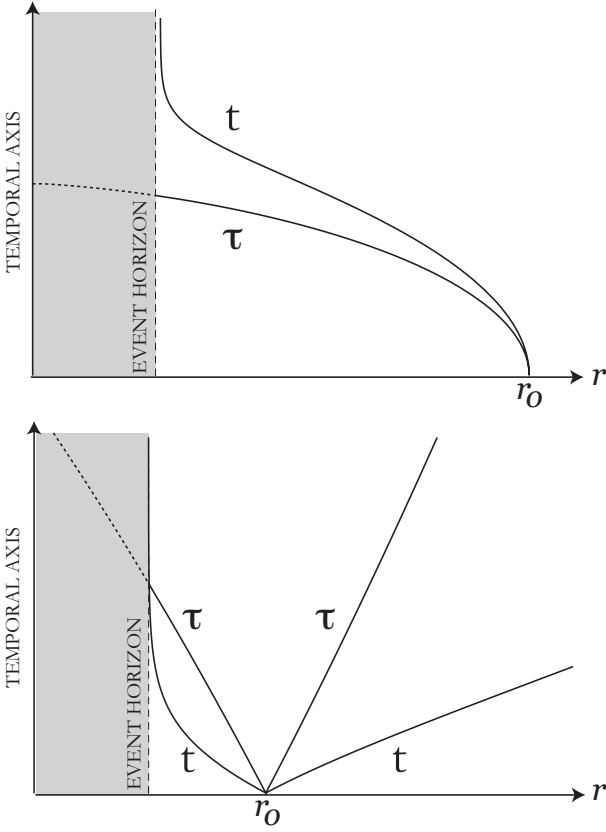


**Fig. 4** Temporal graphic for the fall of radial charged particles in the classic domain. Basically, the behavior is the same as in the standard spacetimes of general relativity [7]. Top panel: Bounded trajectory with  $E_+ < E < m$ . Bottom panel: Unbounded trajectory with  $E = m$ . For convenience, in both graphics we have used the same starting point,  $r_0$ .

respectively. Therefore, as we have mentioned before, the motion of charged particles is the same as the motion in Einstein's spacetimes, see bottom panel of Fig. 4.

## 4.2 The electric domain

### 4.2.1 Frontal Rutherford scattering: $|q_*| < 1$ and $m < E < E_u$

As we have said, the GMGHS spacetime allows a Rutherford-like scattering of radial charged particles. Thus, if the energy particle  $E$  is such that  $m < E < E_u$ , then there are two turning points, one on each side of  $\rho_u$ . Thus, the turning point  $\rho_d > \rho_u$  corresponds to a radial distance of closest approach at the trajectory, whereas  $\rho_a < \rho_u$  is the farthest distance for this interval, see Fig. 2. Explicitly, these distances are given by

$$\rho_d = \frac{q(E - mq_*)}{E^2 - m^2} \left( 1 + \sqrt{1 - \frac{E^2 - m^2}{(E - mq_*)^2}} \right), \quad (27)$$

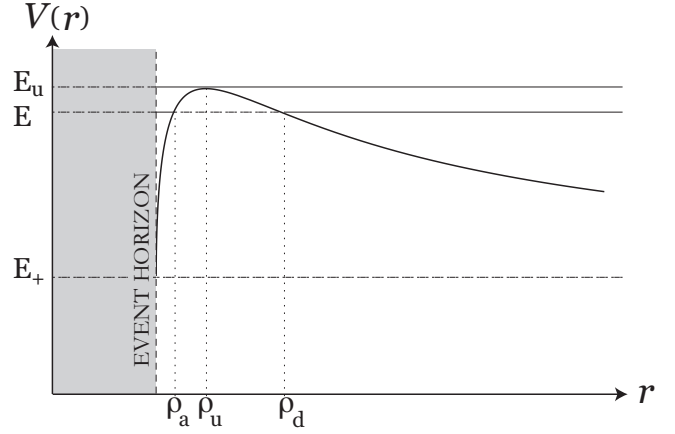


**Fig. 5** Plot of the effective potential for radial charged particles in the electric domain. A frontal Rutherford scattering is allowed when  $E_+ < E < E_u$  and  $r > \rho_d$ , while a critical radial motion occurs when  $E = E_u$ .

and

$$\rho_a = \frac{q(E - mq_*)}{E^2 - m^2} \left( 1 - \sqrt{1 - \frac{E^2 - m^2}{(E - mq_*)^2}} \right). \quad (28)$$

Therefore, Eq. (17) can be rewritten as

$$u^2(r) = \frac{E^2 - m^2}{r^2} h_2(r), \quad (29)$$

where the polynomial is given by  $h_2(r) = |r - \rho_d| |r - \rho_a|$ . Assuming that  $t = \tau = 0$  at the turning point, and defining the radial function  $f(r) = \frac{1}{2} [(r - \rho_d) + (r - \rho_a)]$ , we found that in the proper system

$$\tau(r) = \frac{\sqrt{h_2(r)} + f(0) \log \left( \frac{\sqrt{h_2(r)} + f(r)}{\frac{1}{2}(\rho_d - \rho_a)} \right)}{\sqrt{E^2 - m^2}} \quad (30)$$

while an external observer will measure

$$t(r) = \left[ E + \left( \frac{E}{E_+} - 1 \right) \right] \tau(r) + \tilde{\mathcal{F}}(r), \quad (31)$$

where

$$\tilde{\mathcal{F}}(r) = a \left( \frac{E}{E_+} - 1 \right) \left[ \frac{r_+}{\sqrt{h_2(r_+)}} \log \left( \frac{(r - r_+) f(\rho_d)}{r_+ r + \rho_d \rho_a - (r + r_+) f(0)} \right) - \frac{\sqrt{h_2(r)}}{f(0)} \right], \quad (32)$$

for  $\rho_d < r < \infty$ . In Fig. 6 the proper and external temporal behavior is represented.

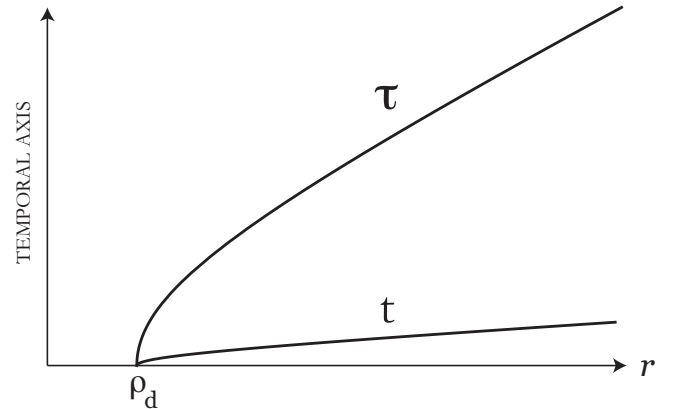


**Fig. 6** Temporal behavior for charged particles in the frontal Rutherford scattering. Here  $\rho_d$  represents the distance of closest approach.

#### 4.2.2 critical radial motion : $|q_*| < 1$ and $E = E_u$

Particles with energy  $E_u$  satisfying the condition  $E_u = V(\rho_u)$ , where  $\rho_u$  is the location of the maximum of the effective potential, see Fig. 5, can arrive to  $\rho_u$  either from a distance  $\rho_i^I < \rho_u$  (region I) or  $\rho_i^{II} > \rho_u$  (region II), depending on its initial velocity. Eventually, if the initial conditions are reversed, charged particles can also arrive to the spatial infinity or the event horizon. Under these assumptions, and then integrating the equations of motion, we obtain for the proper time

$$\tau_I(r) = \pm \frac{1}{\sqrt{E_u^2 - m^2}} [\rho_u \ln A_I(r) - (r - \rho_i^I)], \quad (33)$$

and

$$\tau_{II}(r) = \pm \frac{1}{\sqrt{E_u^2 - m^2}} [(r - \rho_i^{II}) - \rho_u \ln A_{II}(r)], \quad (34)$$

while the coordinate time result to be

$$t_I(r) = E_u \tau_I \pm \frac{q}{\sqrt{E_u^2 - m^2}} \left( \frac{E_u}{E_+} - 1 \right) \ln \frac{A_I^{1+\beta}(r)}{B_I^\beta(r)} \quad (35)$$

and

$$t_{II}(r) = E_u \tau_{II}(r) \mp \frac{q}{\sqrt{E_u^2 - m^2}} \left( \frac{E_u}{E_+} - 1 \right) \ln \frac{A_{II}^{1+\beta}(r)}{B_{II}^\beta(r)} \quad (36)$$

where we have made  $\beta = r_+ / (\rho_u - r_+)$ , and

$$A_I(r) = \frac{\rho_u - \rho_i^I}{\rho_u - r}, \quad B_I(r) = \frac{\rho_i^I - r_+}{r - r_+}, \quad (37)$$

$$A_{II}(r) = \frac{\rho_i^{II} - \rho_u}{r - \rho_u}, \quad B_{II}(r) = \frac{\rho_i^{II} - r_+}{r - r_+}, \quad (38)$$

In Fig. 7 the analytical solutions (33, 34, 35, 36) are depicted. Clearly, an external observer will see the particles going to  $\rho_u$  and spatial infinity faster than in the proper system, while the motion on the horizon possesses the same nature as Einstein's spacetimes, i. e., with respect to an observer stationed at infinite, the trajectory will take an infinite time to reach the horizon even though by its own proper time it will cross the horizon in a finite time [7].

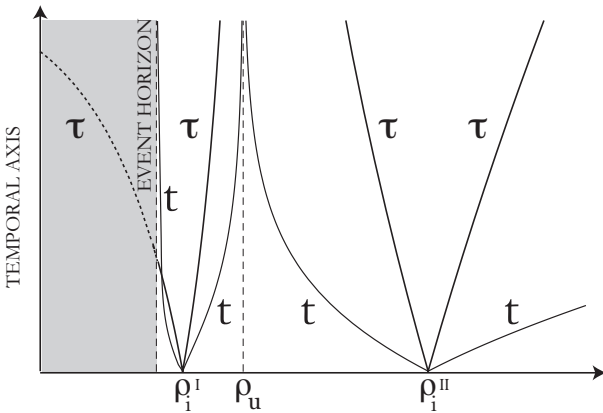


**Fig. 7** Temporal behaviour for charged particles in critical radial motion, where its energy is  $E_u = V(\rho_u)$  and the starting point can be placed at left,  $\rho_i^I$ ) or right of the unstable equilibrium point. Note that in both frames (proper and coordinate) particles arrive asymptotically to  $\rho_u$ .

## 5 Motion with angular momentum

Particles with angular motion are characterized by  $L > 0$ . Explicitly, the effective potential (11) can be written as

$$V(r) = \frac{q}{r} + \sqrt{\left(1 - \frac{r_+}{r}\right) \left(m^2 + \frac{L^2}{r(r-\alpha)}\right)}, \quad (39)$$

which is showed in Fig. 8 for two pairs of value of the electric charge  $q$  and angular momentum  $L$  of the test particle.

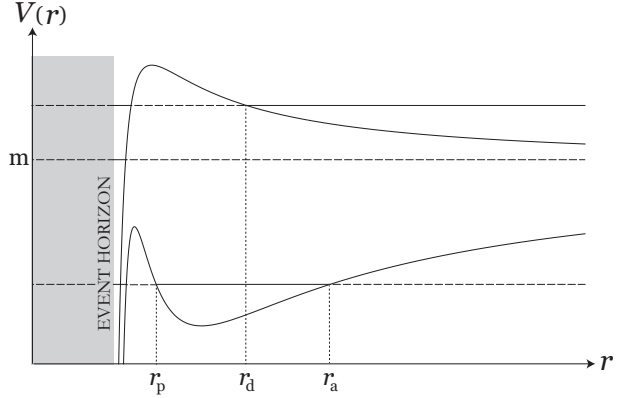


**Fig. 8** Effective potential for charged particles with non-vanished angular momentum. This plot contain curves for two pairs of value of the electric charge  $q$  and angular momentum  $L$  of the test particle. The upper curve corresponds to the typical case of dispersion in which the trajectory approaches from infinity, reaches the turning point  $r_d$ , and then recedes to infinity again.

### 5.1 Gravitational Rutherford scattering

Since the particle interacts with the background via the presence of the term  $\alpha$ , the straight path is modified in such way that a new trajectory is formed. As Fig. 8 illustrate, particles with  $E > m$  are deflected by reaching the distance of closest approach denoted by  $r_d$ . Obviously, without the  $\alpha$  term the geometry becomes the Schwarzschild one, and its counterpart does not exit (we put the interaction "off"). Moreover, a similar effect can occur when the ratio  $L/M$  increases, i.e., tending to the Newtonian regime (see pp. 102 of Chandrasekhar's book [7]).

In order to obtain the mentioned trajectory, let us rewrite Eq. (14) as

$$\phi = \frac{L}{\sqrt{E^2 - m^2}} \int_{r_d}^r \frac{dr}{\sqrt{(r-\alpha)P(r)}}. \quad (40)$$

Here the characteristic polynomial  $P(r)$  is given by

$$P(r) = r^3 - (r_\sigma + \alpha)r^2 - (r_L^2 - \alpha r_\sigma)r + R_L r_L^2, \quad (41)$$

where

$$r_\sigma = \frac{2qE - m^2 r_+}{E^2 - m^2}, R_L = \left( \frac{L^2 r_+ - \alpha q^2}{L^2 - q^2} \right), r_L = \sqrt{\frac{L^2 - q^2}{E^2 - m^2}}. \quad (42)$$

The condition  $P(r) = 0$  allows three real roots, which can be written as

$$r_d(E) = r_\alpha + R \cos \zeta, \quad (43)$$

$$r_A(E) = r_\alpha - \frac{R}{2}(\cos \zeta - \sqrt{3} \sin \zeta), \quad (44)$$

$$r_3(E) = r_\alpha - \frac{R}{2}(\cos \zeta + \sqrt{3} \sin \zeta), \quad (45)$$

where

$$r_\alpha = \frac{r_\sigma + \alpha}{3}, \quad R = \sqrt{\frac{\eta_2}{3}}, \quad \zeta = \frac{1}{3} \arccos \frac{\eta_3}{R^3}, \quad (46)$$

and

$$\eta_2 = 4 \left[ \frac{(r_\sigma + \alpha)^2}{3} + (r_L^2 - \alpha r_\sigma) \right], \quad (47)$$

$$\eta_3 = 4 \left[ \frac{2(r_\sigma + \alpha)^3}{27} + \frac{(r_\sigma + \alpha)(r_L^2 - \alpha r_\sigma)}{3} - R_L r_L^2 \right]. \quad (48)$$

Therefore, we can identify the closest approach distance  $r_d$ , and the farthest distance  $r_A$  (the third solution  $r_3$  is without importance here). Replacing  $P(r) = (r - r_d)(r - r_A)(r - r_3)$  in Eq. (40) and performing an integration it is possible to find that

$$\kappa \phi = \wp^{-1} \left[ \frac{1}{4} \left( \frac{1}{r - r_d} + \frac{a_1}{3} \right); g_2, g_3 \right], \quad (49)$$

where  $\kappa = 2\sqrt{E^2 - m^2}/L$  and  $\wp^{-1}(x; g_2, g_3)$  is the inverse  $\wp$ -Weierstrass elliptic function with the Weierstrass invariant given by

$$g_2 = \frac{1}{4} \left( \frac{1}{3} a_1^2 - a_2 \right), \quad (50)$$

$$g_3 = \frac{1}{16} \left( \frac{1}{3} a_1 a_2 - \frac{2}{27} a_1^3 - a_3 \right), \quad (51)$$

where  $a_1 = u_1 + u_2 + u_3$ ,  $a_2 = u_1 u_2 + u_1 u_3 + u_2 u_3$ ,  $a_3 = u_1 u_2 u_3$ , with  $u_1 = (r_d - \alpha)^{-1}$ ,  $u_2 = (r_d - r_A)^{-1}$ , and  $u_3 = (r_d - r_3)^{-1}$ . Therefore, the inversion of Eq. (49) and a brief manipulation leads to the following expression for the polar trajectory

$$r(\phi) = r_d + \frac{1}{4\wp(\kappa\phi; g_2, g_3) - a_1/3}, \quad (52)$$

where  $\wp(x; g_2, g_3)$  is the  $\wp$ -Weierstrass elliptic function. In Fig. 9 we plot the polar trajectory (52), in which we note that, depending on the set of parameters  $(E, L, q, \alpha)$  across Eqs. (60-48), the trajectory will be deflected as a classic Rutherford scattering [64–70] or more specifically a repulsive or attractive scattering between a massive target (composed of a positive charged nuclei) and light projectiles ( $\alpha$ -particles or  $\beta$ -particles). Moreover, because our test particles have been chosen as positive, the attractive behavior is driven by the gravitational field over the electric repulsion. From the equation of the orbit (49) it is possible to obtain the angle of deflection  $\Theta = 2\phi_\infty - \pi$  experienced by test particles, which turns out to be:

$$\Theta = \frac{2}{\kappa} \wp^{-1} \left( \frac{a_1}{12} \right) - \pi. \quad (53)$$

Therefore, particles with  $E = E_1$  do not experience deflection in their trajectory, where  $E_1$  is the solution to the transcendental equation  $a_1 = 12\wp(\kappa\pi/2)$ .

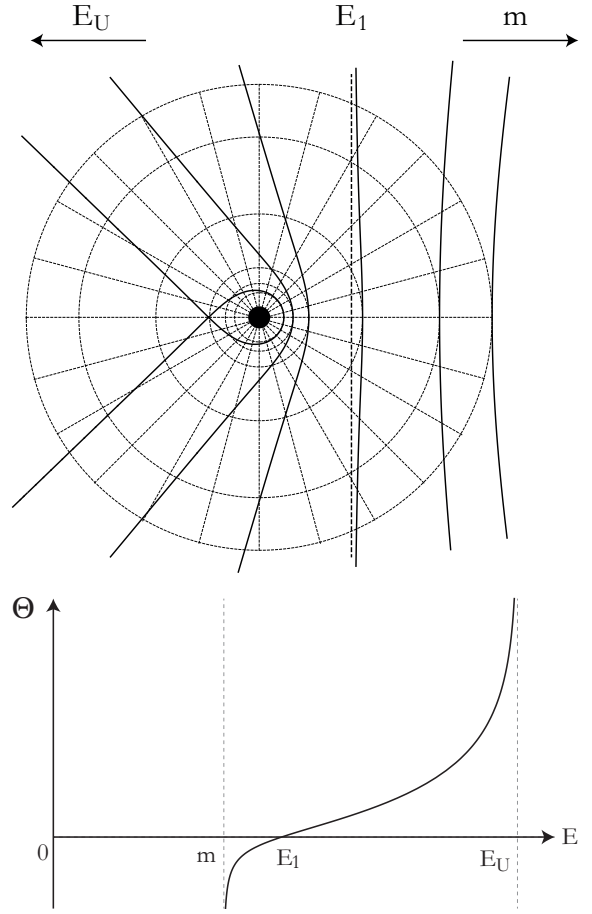


**Fig. 9** Top panel: Gravitational Rutherford scattering. This plot contain curves for various value of the electric charge,  $q$ , and impact parameter,  $b$ , of the test particle. Clearly, depending on the value of  $b$ , the scattering can be either repulsive or attractive. Each circle corresponds to the closest approach distance for a given value of the impact parameter. Bottom panel: Angle of scattering against energy of the test particles. At  $E = E_1$  the deflection angle is equal to zero, so initial and final direction are the same.

Also, a repulsive scattering is performed if  $m < E < E_1$ , whereas an attractive scattering is carried out if  $E_1 < E < E_U$ . For the scattering problem, the dependence of the differential cross-section on  $\Theta \neq 0$  is given by

$$\frac{d\sigma}{d\Omega} \equiv \sigma[\Theta] = \frac{b}{\sin \Theta} \left| \frac{db}{d\Theta} \right|, \quad (54)$$

where  $b$  is the impact parameter. Now, we can substitute the constants  $E$  and  $L$  by the value at spatial infinity as [38]:

$$E = \frac{m}{\sqrt{1 - v^2}}, \quad L = \frac{m v b}{\sqrt{1 - v^2}} = b \sqrt{E^2 - m^2} \quad (55)$$

where  $v$  is the velocity of the test particle at spatial infinity. Because  $b = b(E)$ , then  $a_1 = a_1(b)$  and Eq. (54) is written as

$$\sigma[\Theta] = \frac{b}{\sin \Theta} \left| \frac{da_1}{d\Theta} \right| \left| \frac{db}{da_1} \right|. \quad (56)$$

Finally, the differential cross-section for the scattering of charged particles by the background of a charged black hole in heterotic string theory is given by

$$\sigma[\Theta] = 12 \csc \Theta \left| \wp' \left( \frac{\pi + \Theta}{b} \right) \right| \left| \frac{db}{da_1} \right|, \quad (57)$$

where  $\wp'(x) \equiv \wp'(x, g_2, g_3)$  represents a derivative of the  $\wp$ -Weierstraß function with respect to  $\Theta$ . Note that this last expression represents the exact formula for the scattering problem. Nevertheless, due to the complexity of the relation between the impact parameter  $b$  and the quantity  $a_1$ , the term  $\left| \frac{db}{da_1} \right|$  is calculated numerically.

## 5.2 Keplerian orbits

As we have established, the effective potential (39) allows motion between an *apastron* distance  $r_a$  and *periastron* distance  $r_p$ , as we show in Fig.9. Therefore, considering that  $E < m$ , it is possible to rewrite Eq. (14) as

$$\phi = \frac{L}{\sqrt{m^2 - E^2}} \int_{r_a}^r \frac{dr}{\sqrt{(r - \alpha)\bar{P}(r)}}, \quad (58)$$

where the characteristic polynomial  $\bar{P}(r)$  is now given by

$$\bar{P}(r) = -r^3 + (-\bar{r}_\sigma + \alpha)r^2 - (\bar{r}_L^2 - \alpha\bar{r}_\sigma)r + R_L\bar{r}_L^2, \quad (59)$$

and

$$\bar{r}_\sigma = \frac{2qE - m^2 r_+}{m^2 - E^2}, R_L = \left( \frac{L^2 r_+ - \alpha q^2}{L^2 - q^2} \right), \bar{r}_L = \sqrt{\frac{L^2 - q^2}{m^2 - E^2}}. \quad (60)$$

The condition  $\bar{P} = 0$  allows us to get the three roots which are given by

$$r_p(E) = -\bar{r}_\alpha + \bar{R} \sin \bar{\zeta}, \quad (61)$$

$$r_a(E) = -\bar{r}_\alpha + \frac{\bar{R}}{2}(\sqrt{3} \cos \bar{\zeta} - \sin \bar{\zeta}), \quad (62)$$

$$r_f(E) = -\bar{r}_\alpha - \frac{\bar{R}}{2}(\sqrt{3} \cos \bar{\zeta} + \sin \bar{\zeta}) \quad (63)$$

where

$$\bar{r}_\alpha = \frac{\bar{r}_\sigma - \alpha}{3}, \quad \bar{R} = \sqrt{\frac{\bar{\eta}_2}{3}}, \quad \bar{\zeta} = \frac{1}{3} \arcsin \frac{\bar{\eta}_3}{\bar{R}^3}, \quad (64)$$

and

$$\bar{\eta}_2 = 4 \left[ \frac{(\bar{r}_\sigma - \alpha)^2}{3} - (\bar{r}_L^2 - \alpha\bar{r}_\sigma) \right], \quad (65)$$

$$\bar{\eta}_3 = 4 \left[ \frac{2(\bar{r}_\sigma - \alpha)^3}{27} - \frac{(\bar{r}_\sigma - \alpha)(\bar{r}_L^2 - \alpha\bar{r}_\sigma)}{3} - R_L\bar{r}_L^2 \right]. \quad (66)$$

Defining  $\kappa_{kep} = 2\sqrt{m^2 - E^2}/L$  and then integrating Eq. (58) we get that

$$\kappa_{kep} \phi = \wp^{-1} \left[ \frac{1}{4} \left( \frac{1}{r_a - r} - \frac{\bar{a}_1}{3} \right); \bar{g}_2, \bar{g}_3 \right], \quad (67)$$

where the Weierstraß invariants are given by

$$\bar{g}_2 = \frac{1}{4} \left( \frac{1}{3} \bar{a}_1^2 - \bar{a}_2 \right), \quad (68)$$

$$\bar{g}_3 = \frac{1}{16} \left( \frac{1}{3} \bar{a}_1 \bar{a}_2 - \frac{2}{27} \bar{a}_1^3 - \bar{a}_3 \right), \quad (69)$$

where  $\bar{a}_1 = \bar{u}_1 + \bar{u}_2 + \bar{u}_3$ ,  $\bar{a}_2 = \bar{u}_1\bar{u}_2 + \bar{u}_1\bar{u}_3 + \bar{u}_2\bar{u}_3$ ,  $\bar{a}_3 = \bar{u}_1\bar{u}_2\bar{u}_3$  and  $\bar{u}_1 = (r_a - \alpha)^{-1}$ ,  $\bar{u}_2 = (r_a - r_p)^{-1}$ ,  $\bar{u}_3 = (r_a -$

$r_f)^{-1}$ . Therefore, the polar trajectory can be found inverting the Eq. (67), which results to be

$$r(\phi) = r_a - \frac{1}{4\wp(\kappa_{kep} \phi; \bar{g}_2, \bar{g}_3) + \bar{a}_1/3}. \quad (70)$$

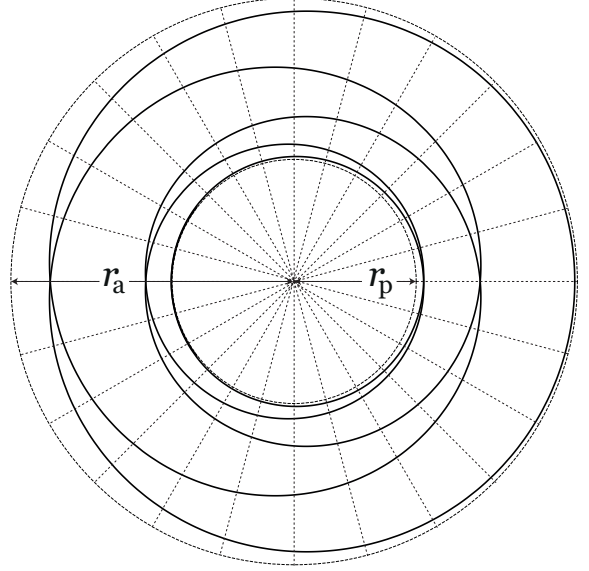


**Fig. 10** Polar plot for Keplerian orbit performed by charged particles in which the precession angle is given by Eq. (71).

In Fig. 10 we depict the Keplerian orbit in which the precession angle,  $\Xi = 2\phi_p - 2\pi$ , is given by

$$\Xi = \frac{2}{\kappa_{kep}} \wp^{-1} \left[ \frac{1}{4} \left( \frac{1}{r_a - r_p} - \frac{\bar{a}_1}{3} \right), \bar{g}_2, \bar{g}_3 \right] - 2\pi. \quad (71)$$

## 6 Final remarks

In this paper, we have examined the motion of charged particles in the background metric and the fields of a GMGHS black hole. The motion equations were established and solved exactly following the usual Hamilton–Jacobi method. Thus, the radial motion of test bodies was studied in terms of its energy  $E$  and specific charge  $q_*$ , allowing two regimens: *the classic domain* is similar to the radial motion studied in the Schwarzschild spacetimes, thereby allowing bounded trajectories ( $|q_*| > 1$  and  $E_+ < E < m$ ) and unbounded trajectories ( $|q_*| \leq 1$  and  $E \geq m$ ); and *the electric domain*, in which case a frontal repulsive Rutherford scattering is permitted ( $|q_*| < 1$  and  $m < E < E_u$ ) together with a critical motion in which a particle *falls* asymptotically into  $\rho_u$  ( $|q_*| < 1$  and  $E = E_u$ ). On the other hand, the motion with non-vanished angular momentum was studied in detail in two general schemes: the dispersive case  $E > m$  and the Keplerian case  $E < m$ . In the first case, we employed the classic tools to describe the Rutherford scattering between two electric charges (with the same sign of the charge), showing that null dispersion and attractive scattering are possi-



ble because the electric dispersion is compensated by the gravitational effects. Finally, for the second case, we have calculated the apastron and periastron distance of the Keplerian orbit, which is expressed in terms of the elliptic  $\wp$ -Weierstraß function, whose periastron advance with a precession angle  $\Xi$  is given by Eq. (71).

**Acknowledgements** This work was funded by the Comisión Nacional de Investigación Científica y Tecnológica through FONDECYT Grants No 11130695.

## References

1. A. Einstein, *Erklärung der perihelbewegung des Merkur aus der allgemeinen relativitätstheorie*, Sitzungsberichte der Königlich Preußische Akademie der Wissenschaften, 831–839 (1915).
2. A. Einstein, *Die Grundlage der allgemeinen Relativitätstheorie*, Ann. Phys. **354**, 769–822 (1916).
3. F.W. Dyson, A.S. Eddington and C. Davidson, *A determination of the deflection of light by the Sun's gravitational field, from observations made at the total eclipse of 29 May 1919*, Philosophical Transactions of the Royal Society **220 A**, 291–333 (1920).
4. G.M. Clemence, *The relativity effect in planetary motions*, Rev. Mod. Phys. **19** (4), 361–364 (1947).
5. I.I. Shapiro, *Solar system tests of general relativity: recent results and present plans, general relativity and gravitation*, 1st ed. Cambridge: Cambridge University Press, 313–330. (1990).
6. C.W. Will, *The confrontation between general relativity and experiment*, Living Rev. Rel. **9**, 3 (2006) [arXiv:1403.7377 [gr-qc]].
7. S. Chandrasekhar, *The mathematical theory of black holes*, Oxford University Press, New York (1983).
8. F. Kottler, *Über die physikalischen grundlagen der Einsteinschen gravitationstheorie*, Ann. Phys. **56**, 410 (1918).
9. M.J. Jaklitsch, C. Hellaby and D.R. Matravers, *Particle motion in the spherically symmetric vacuum solution with positive cosmological constant*, Gen. Rel. Grav. **21**, 941 (1989).
10. Z. Stuchlík and M. Calvani, *Null geodesics in black hole metrics with non-zero cosmological constant*, Gen. Rel. Grav. **23**, 507 (1991).
11. Z. Stuchlík and S. Hledík, *Some properties of the Schwarzschild–de Sitter and Schwarzschild–anti–de Sitter spacetimes*, Phys. Rev. D **60**, 044006 (1999).
12. J. Podolsky, *The Structure of the extreme Schwarzschild–de Sitter spacetime*, Gen. Rel. Grav. **31**, 1703 (1999) [arXiv:9910029 [gr-qc]].
13. G.V. Kraniotis and S.B. Whitehouse, *Exact calculation of the perihelion precession of mercury in general relativity, the cosmological constant and jacobi's inversion problem*, Class. Quantum Grav. **20**, 4817 (2003) [arXiv:0305181 [astro-ph]].
14. G.V. Kraniotis, *Precise relativistic orbits in Kerr spacetime with a cosmological constant*, Class. Quantum Grav. **21**, 4743 (2004) [arXiv:0405095 [gr-qc]].
15. N. Cruz, M. Olivares and J.R. Villanueva, *The geodesic structure of the Schwarzschild anti–de Sitter Black Hole*, Class. Quantum Grav. **22**, 1167 (2005) [arXiv:0408016 [gr-qc]].
16. E. Hackmann and C. Lammerzahl, *Geodesic equation in Schwarzschild–(anti–) de Sitter spacetimes: Analytical solutions and applications*, Phys. Rev. D **78**, 024035 (2008) [arXiv:1505.07973 [gr-qc]].
17. E. Hackmann and C. Lammerzahl, *Complete analytic solution of the geodesic equation in Schwarzschild–(anti–) de Sitter spacetimes*, Phys. Rev. Lett. **100**, 171101 (2008) [arXiv:1505.07955 [gr-qc]].
18. J.R. Villanueva, J. Saavedra, M. Olivares and N. Cruz, *Photons motion in charged Anti–de Sitter black holes*, Astrophys. Space Sci. **344**, 437 (2013).
19. Z. Stuchlík and S. Hledík, *Properties of the Reissner–Nordström spacetimes with a nonzero cosmological constant*, Acta Phys. Slov. **52**, 363 (2002) [arXiv:0803.2685 [gr-qc]].
20. D. Pugliese, H. Quevedo and R. Ruffini, *Circular motion of neutral test particles in Reissner–Nordström spacetime*, Phys. Rev. D **83**, 024021 (2011) [arXiv:1012.5411 [gr-qc]].
21. E. Hackmann, V. Kagramanova, J. Kunz and C. Lammerzahl, *Analytic solutions of the geodesic equation in higher dimensional static spherically symmetric spacetimes*, Phys. Rev. D **78**, 124018 (2008) [arXiv:0812.2428 [gr-qc]].
22. R. Fujita and W. Hikida, *Analytical solutions of bound timelike geodesic orbits in Kerr spacetime*, Class. Quantum Grav. **26**, 135002 (2009) [arXiv:0906.1420 [gr-qc]].
23. Z. Stuchlík and P. Slany, *Equatorial circular orbits in the Kerr–de Sitter spacetimes*, Phys. Rev. D, **69**, 064001 (2004) [arXiv:0307049 [gr-qc]].
24. D. Pugliese, H. Quevedo and R. Ruffini, *Equatorial circular orbits of neutral test particles in the Kerr–Newman spacetime*, Phys. Rev. D **88**, 024042 (2013) [arXiv:1303.6250 [gr-qc]].
25. S. Pireaux, *Light deflection in Weyl gravity: Critical distances for photon paths*, Class. Quant. Grav. **21** 1897–1913 (2004) [arXiv:0403071 [gr-qc]].
26. S. Pireaux, *Light deflection in Weyl gravity: Constraints on the linear parameter*, Class. Quant. Grav. **21** 4317–4334 (2004) [arXiv:0408024 [gr-qc]].
27. J. Sultana and D. Kazanas, *Bending of light in conformal Weyl gravity*, Phys. Rev. D **81** 127502 (2010).
28. J. Sultana, D. Kazanas and J. L. Said, *Conformal Weyl Gravity and perihelion precession*, Phys. Rev. D **86**,

- 084008 (2012).
29. J.R. Villanueva and M. Olivares, *On the null trajectories in conformal Weyl gravity*, J. Cosmol. Astropart. Phys. **06**, 040 (2013) [arXiv:1305.3922 [gr-qc]].
  30. J. Chen and Y. Wang, *Timelike geodesic motion in Hořava–Lifshitz spacetime*, Int. J. Mod. Phys. A **25**, 1439 (2010) [arXiv:0905.2786 [gr-qc]].
  31. M. Olivares, G. Rojas, Y. Vásquez and J.R. Villanueva, *Particles motion on topological Lifshitz black holes in 3+1 dimensions*, Astrophys. Space Sci. **347**, 83-89 (2013) [arXiv:1304.4297 [gr-qc]].
  32. N. Cruz, M. Olivares and J.R. Villanueva, *Geodesic structure of the Lifshitz black hole in 2+1 dimensions*, Eur. Phys. J. C **73**, 2485 (2013). [arXiv:1305.2133 [gr-qc]].
  33. J.R. Villanueva and Y. Vásquez, *About the coordinate time for photons in Lifshitz spacetimes*, Eur. Phys. J. C **73**, 2587 (2013) [arXiv:1309.4417 [gr-qc]].
  34. M. Olivares, Y. Vásquez, J.R. Villanueva and F. Moncada, *Motion of particles on a  $z = 2$  Lifshitz black hole background in 3+1 dimensions*, Celest. Mech. Dyn. Astr. **119**, 207 (2014) [arXiv:1306.5285 [gr-qc]].
  35. S. Zhou, J. Chen and Y. Wang, *Geodesic structure of test particle in Bardeen spacetime*, Int. J. Mod. Phys. D **21** 9, 1250077 (2012) [arXiv:1112.5909 [gr-qc]].
  36. M. Halilsoy, O. Gurtug and S. Habib Mazharimousavi, *Rindler modified Schwarzschild geodesics*, Gen. Rel. Grav. **45** 11, 2363 (2013) [arXiv:1312.5574 [gr-qc]].
  37. C. Leiva, J. Saavedra and J.R. Villanueva, *The geodesic structure of the Schwarzschild black holes in gravity's Rainbow*, Mod. Phys. Lett. A **24**, 1443-1451 (2009) [arXiv:0808.2601 [gr-qc]].
  38. T. Maki and K. Shiraiishi, *Motion of test particles around a charged dilatonic black hole*, Class. Quantum Grav. **11**, 227 (1994).
  39. E. Hackmann, B. Hartmann, C. Lämmerzahl and P. Sirimachan, *The complete set of solutions of the geodesic equations in the spacetime of a Schwarzschild black hole pierced by a cosmic string*, Phys. Rev. D **81**, 064016 (2010) [arXiv:0912.2327 [gr-qc]].
  40. B. Hartmann and P. Sirimachan, *Geodesic motion in the spacetime of a cosmic string*, J. High Energy Phys. **1008**, 110 (2010) [arXiv:1007.0863 [gr-qc]].
  41. A. Bhadra, *Gravitational lensing by a charged black hole of string theory*, Phys. Rev. D **67**, 103009 (2003) [arXiv:0306016 [gr-qc]].
  42. A.R. Prasanna and R.K. Varma, *Charged particle trajectories in a magnetic field on a curved spacetime*, Pramana **8** 3, 229 (1977).
  43. A.R. Prasanna and S. Sengupta, *Charged particle trajectories in the presence of a toroidal magnetic field on a Schwarzschild background*, Phys. Lett. A **193**, 25 (1994).
  44. N. Dadhich, C. Hoenselaers and C.V. Vishveshwara, *Trajectories of charged particles in the static Ernst space-time*, J. Phys. A: Math. Gen. **12**, 215 (1979).
  45. J. Bičák and Z. Stuchlík and V. Balek, *The motion of charged particles in the field of rotating charged black holes and naked singularities. I.- The general features of the radial motion and the motion along the axis of symmetry*, Bull. Astron. Inst. Czechosl. **40** 2, 65 (1989).
  46. V. Balek, J. Bičák and Z. Stuchlík, *The motion of charged particles in the field of rotating charged black holes and naked singularities. II.- The motion in the equatorial plane*, Bull. Astron. Inst. Czechosl. **40** 3, 133 (1989).
  47. V.D. Gladush and M.V. Galadgyi, *General-relativistic radial motions of neutral and charged test particles in the field of a charged spherically symmetric object*, Kinemat. Phys. Celest. Bodies, **25** 2, 79 (2008).
  48. S. Grunau and V. Kagramanova, *Geodesics of electrically and magnetically charged test particles in the Reissner-Nordström space-time: analytical solutions*, Phys. Rev. D **83**, 044009 (2011) [arXiv:1011.5399 [gr-qc]].
  49. J.M. Cohen and R. Gautreau, *Naked singularities, event horizons, and charged particles*, Phys. Rev. D **19** 8, 2273 (1979).
  50. D. Pugliese, H. Quevedo and R. Ruffini, *Motion of charged test particles in Reissner-Nordström spacetime*, Phys. Rev. D **83**, 104052 (2011) [arXiv:1103.1807 [gr-qc]].
  51. M. Olivares, J. Saavedra, C. Leiva and J.R. Villanueva, *Motion of charged particles on the Reissner-Nordström (Anti)-de Sitter black hole spacetime*, Mod. Phys. Lett. A **26**, 2923 (2011) [arXiv:1101.0748 [gr-qc]].
  52. A.N. Aliev and N. Özdemir, *Motion of charged particles around a rotating black hole in a magnetic field*, Mon. Not. R. Astron. Soc. **336**, 241 (2002) [arXiv:0208025 [gr-qc]].
  53. A.A. Abdujabbarov, B.J. Ahmedov and N.B. Jurayeva, *Charged-particle motion around a rotating non-Kerr black hole immersed in a uniform magnetic field*, Phys. Rev. D **87**, 064042 (2013).
  54. M. Takahashi and H. Koyama, *Chaotic motion of charged particles in an electromagnetic field surrounding a rotating black hole*, Astrophys. J. **693**, 472 (2009) [arXiv:0807.0277 [astro-ph]].
  55. E. Hackmann and H. Xu, *Charged particle motion in Kerr–Newmann spacetimes*, Phys. Rev. D **87**, 124030 (2013) [arXiv:1304.2142 [gr-qc]].
  56. S. Fernando, *Null geodesics of charged black holes in string theory*, Phys. Rev. D **85**, 024033 (2012). [arXiv:1109.0254 [gr-qc]].
  57. M. Olivares and J.R. Villanueva, *Massive neutral particles on heterotic string theory*, Eur. Phys. J. C **73**, 2659 (2013) [arXiv:1311.4236 [gr-qc]].

- 
58. C. Blaga, *Circular time-like geodesics around a charged spherically symmetric dilaton black hole*, *Automat. Comp. Appl. Math.* **22**, 41-48 (2013) [arXiv:1406.7421 [gr-qc]].
59. C. Blaga, *Timelike geodesics around a charged spherically symmetric dilaton black hole*, *Serb. Astron. J.* **190**, 41 (2015) [arXiv:1407.1504 [gr-qc]].
60. A. Sen, *Rotating Charged Black Hole Solution in Heterotic String Theory*, *Phys. Rev. Lett.* **69**, 7 (1992) [arXiv:9204046 [gr-qc]].
61. S.F. Hassan and A. Sen, *Twisting classical solutions in heterotic string theory*, *Nucl. Phys. B* **375**, 103 (1992) [arXiv:9109038 [gr-qc]].
62. G.W. Gibbons and K. Maeda, *Black holes and membranes in higher dimensional theories with dilaton fields*, *Nucl. Phys. B* **298**, 741 (1988).
63. D. Garfinkle, G.T. Horowitz and A. Strominger *Charged black holes in string theory*, *Phys. Rev. D* **43**, 3140 (1991).
64. H. Geiger, *On the scattering of  $\alpha$ -particles by matter*, *Proc. R. Soc. Lond. A* **81** 546, 174 (1908).
65. H. Geiger, *The scattering of the  $\alpha$ -particles by matter*, *Proc. R. Soc. Lond. A* **83** 565, 492 (1910).
66. H. Geiger and E. Marsden, *The laws of deflexion of  $\alpha$ -particles through large angles*, *Phil. Mag. Series 6* **25** 148, 604 (1913).
67. E. Rutherford, *The scattering of  $\alpha$  and  $\beta$  particles by matter and the structure of the atom*, *Phil. Mag. Series 6* **21** 669 (1911).
68. E. Rutherford, *The origin of  $\beta$  and  $\gamma$  rays from radioactive substances*, *Phil. Mag. Series 6* **24** 142, 453 (1912).
69. E. Rutherford and J.M. Nuttal, *Scattering of  $\alpha$ -particles by gases*, *Phil. Mag. Series 6* **26** 154, 702 (1913).
70. E. Rutherford, *The structure of the atom*, *Phil. Mag. Series 6* **27** 159, 488 (1914).